Graduation Internship Report

RF Hydrogen Plasma Diagnostics

Author:
C.P.E.C. Geluk
Student ID:
10086781

ASML The Netherlands
Supervisor:
Dr. D. Smeets

The Hague University of Applied Sciences
Supervisor:
Mw. drs. M.C. Vloemans

December 18, 2012

Abstract

The characteristics of a hydrogen plasma in an inductively coupled RF plasma setup were studied using a double Langmuir probe and an optical emission spectrometer. At various settings for the gas pressure, gas flow, RF power and probe position, values were obtained for the electron temperature and plasma density. Additionally, the hydrogen dissociation degree was measured inside the discharge. In the discharge, the maximum electron temperature is (3.9±0.5) eV at 300 W, 5.0 Pa. This value decreases by 0.5 - 1 eV when the power is decreased or when the pressure is increased. At distances up to 90 mm from the discharge, the electron temperature also decreases by 0.5 - 1 eV. The plasma density inside the discharge depends linearly on power, but is independent of pressure (between 5.0 and 35.0 Pa) at $(1.0^{+0.2}_{-0.4}) \cdot 10^{17}$ m^{-3} for $P = 300$ W. Away from the discharge there is still a plasma, but the density decreases exponentially, depending on the pressure by 2 (at 5.0 Pa) to 3 (at 35.0 Pa) orders of magnitude at 90 mm from the discharge. The degree of dissociation in the discharge lies between $(1.5 \pm 0.4)\%$ at 5.0 Pa and $(0.8 \pm 0.4)\%$ at 35.0 Pa for 300 W RF power. The atomic hydrogen density increases with background pressure and is maximum at $(7 \pm 3) \cdot 10^{19}$ m^{-3} at 35 Pa, 300 W. No changes in the plasma were observed upon changes of the hydrogen flow between 20 and 60 sccm.

Contents

Chapter 1

Introduction

ASML is one of the world's leading providers of lithography systems for the semiconductor industry, manufacturing complex machines that are critical to the production of integrated circuits or chips. ASML customers continuously seek ways of improving chip performance, for instance by decreasing transistor sizes, allowing more transistors to be packed onto a substrate. While current optical lithography systems use a 193 nm light source for the projection of patterns, next-generation machines will be using light in the Extreme Ultraviolet (EUV) regime. EUV lithography systems use light sources of 13.5 nm wavelength.

The use of this type of light source creates many different challenges. For example, EUV is absorbed by many substances, including air and glass. This means the complete system is operated at vacuum and glass lenses can no longer be used and need to be replaced by multilayer mirrors.

Various gases may be purged into the system. Under influence of the EUV photons (which carry approximately 92 eV of energy at 13.5 nm), a plasma could be formed. Energetic ions or neutrals of a plasma may cause damage to the cap layers of the multilayer mirrors, degrading them up to the point that the mirrors lose too much reflection. This is mainly relevant in the EUV source, where EUV intensities and gas pressure are relatively high.

In order to develop cap layer materials that are not affected by the presence of a plasma, a plasma setup was built. In this setup, an Inductively Coupled Plasma (ICP) is created. Plasma settings can easily be adjusted, allowing for the creation of a plasma environment that is best suited to test various materials. The goal is to create a recipe for a plasma exposure of test samples which is comparable to exposure to source conditions for an extended amount of time. This study will focus on the diagnostics of a hydrogen plasma in this setup.

Chapter 2

Plasma & Diagnostics Theory

2.1 Plasma Theory

2.1.1 Plasma General

Next to the three 'classical' states of matter (solid, liquid and gas), a fourth state of matter is known as plasma. A plasma is basically a gas in which a fraction of the molecules or atoms is ionized. Ionization may be caused by high temperatures or the presence of a large electric field. Although a plasma is much like a gas, plasma behaviour is very different to gas behaviour due te presence of charged particles.

The two most characteristic properties of a plasma are the electron density n_e (m^{-3}) and electron temperature T_e (K). For convenience, the electron temperature is usually expressed as $\bar{T}_e$ (eV), with:

$$1 \text{ eV} = 1 \cdot \frac{k_{\mathrm{B}}}{-q_e} = 11.6 \cdot 10^3 \text{ K} \tag{2.1}$$

where $k_{\mathrm{B}} = 1.38 \cdot 10^{-23}$ (J·K^{-1}) and $q_e = -1.60 \cdot 10^{-19}$ (C) being the Boltzmann constant and electron charge, respectively.

While particles in a plasma interact kinetically like in a gas, there is also interaction due to the electrical charge of electrons and ions. In most laboratory plasma circumstances, the kinetic interaction is much stronger than the electrical interaction. Such 'weakly coupled' plasmas are quasi-neutral: the ion density is equal to the electron density and can simply be denoted plasma density, or $n_{\mathrm{i}} = n_e = n$. [1]

When the plasma is powered by a DC power source, ions and electrons acquire levels of kinetic energy of the same order of magnitude. However, when an AC power source with a frequency above 100 kHz is used, the alternating fields cannot speed up the relatively heavy ions anymore. Only electrons are sufficiently light to respond to these fields. All power is therefore coupled into the plasma by the electrons, which in turn transfer this energy to other species by interacting kinetically and electrically, resulting in dissociation and ionization. Inside the plasma, ion temperatures are typically 100 times lower than electron temperatures. [1] Ions however gain a lot more energy when they are accelerated towards a surface by a sheath. For the purpose of materials processing, ion energy can also be increased by applying a bias voltage to a probe or sample.

2.1.2 Plasma Sheaths

The presence of a conducting object in a plasma environment (e.g., the vessel wall or an electric probe) will induce the creation of a plasma sheath: a region of low electron density between

the plasma and the electrode. Since electrons usually contain more kinetic energy while having less mass, they are much more mobile than ions. Electron are therefore more readily lost to surfaces by diffusion. This leaves a net positive charge in the plasma region, until the plasma restores the charge balance by the creation of a sheath. Due to this sheath, a potential drop exists between the plasma and the electrode of the order of $\bar{T}_e$. Then, all electrons are confined in the plasma region.

The plasma region and the sheath region are joined together by a pre-sheath, across which a small potential difference exists. The pre-sheath accellerates the ions to a certain velocity, called the Bohm velocity, or u_B (m·s^{-1}). This accelleration is the result of ambipolar diffusion, where fast electrons 'drag' ions outwards due to Coulomb forces. While the ion flux remains constant, the ion velocity increases towards the electrode and as a result, the sheath ion density n_s (m^{-3}) is smaller compared to the ion density in the plasma (also called bulk ion density or n_b (m^{-3})) by a factor $e^{-1/2} = 0.61$. [1]

2.1.3 Plasma Expansion

When a plasma is confined in a certain region surrounded by neutral gas, electrons, ions and energetic neutrals will diffuse into the region where no plasma is being created. In this diffusion process, net charges are lost due to recombination (e.g., $e^- + H^+ + e^- \rightarrow H + e^-$ [2]), and kinetic energy is lost in collisions. Also, charge transfer without recombination plays a large role (for instance $H^+ + H \rightarrow H + H^+$ [2]). For the collision rate of a certain flux, the following can be written:

$$d\Gamma = -\sigma \Gamma n_g dx \tag{2.2}$$

where Γ is the ion flux (m^{-2}·s^{-1}), σ is the collision or recombination cross section (m^2), n_g is the neutral gas density (m^{-3}) and x (m) is the distance from the plasma. When the equation above is integrated, the collided flux is calculated to be

$$\Gamma(x) = \Gamma(0) \cdot \left(1 - e^{-x/\lambda}\right) \tag{2.3}$$

with the remaining, uncollided flux:

$$\Gamma(x) = \Gamma(0) \cdot e^{-x/\lambda} \tag{2.4}$$

In Equation 2.3 and 2.4, $\Gamma(0)$ is the flux at distance 0 (the edge of the actively created plasma), and

$$\lambda = \frac{1}{n_g \sigma} \tag{2.5}$$

is the mean free path for the collision or recombination in question. [1]

Since the region between the discharge and the vessel wall is effectively a pre-sheath, the velocity of the ions and electrons in this region is the Bohm velocity u_B.

2.2 Langmuir Probe

Since a plasma contains electrically charged species, it acts as an efficient electric conductor. This property can be used to determine plasma properties, for instance using a Langmuir probe. Most electric probes involving measuring current/voltage characteristics are referred to as Langmuir probes.

A relatively simple probe is a double Langmuir probe. This type of probe consists of two identical metals tips protruding in the plasma. When a voltage is applied across these tips, electrons are attracted to the positive probe and ions are attracted to the negative probe where they recombine with an electron, thereby effectively closing an electrical circuit so a net current can flow. Since electrons are much more mobile than ions, the current is limited by the local ion density.

The current through these tips is measured as a function of the voltage that is applied across the two tips. With this type of probe, the bulk plasma density can be estimated from the saturation current for negative voltages. Electrons are then repelled from the electrode and the current through the probe is a pure ion current:

$$I_\mathrm{i} = -q_e n_\mathrm{s} u_\mathrm{B} A = -q_e n_\mathrm{b} \mathrm{e}^{1/2} u_\mathrm{B} A \tag{2.6}$$

Here, I_i (A) is the ion current, $q_e = 1.6 \cdot 10^{-19}$ (C) is the electron charge, n_s (m^{-3}) is the sheath plasma density which differs from the bulk plasma density $n_\mathrm{b} = n$ (m^{-3}) by a factor $\mathrm{e}^{1/2}$, A (m^3) is the probe area and u_B (m·s^{-1}) is the Bohm velicity, reading:

$$u_\mathrm{B} = \sqrt{\frac{k_\mathrm{B} T_e}{m_\mathrm{i}}} = \sqrt{\frac{q_e \bar{T}_e}{m_\mathrm{i}}} \tag{2.7}$$

where m_i (kg) is the ion mass. Simulations show that H_3^+ is the most abundant ion in low-pressure, low-density plasmas like the one used in this study, so the ion mass is the H_3^+ mass $= 3$ u $= 4.98 \cdot 10^{-27}$ kg. [3] In order to determine n, the electron temperature $\bar{T}_e$ is needed, which is determined by a double Langmuir probe. One measurement is sufficient to obtain both the electron temperature $\bar{T}_e$ and the plasma density n.

For the symmetrical case with identical electrodes, the current-voltage characteristic of $I(V)$-curve is given by:

$$I(V) = I_\mathrm{i} \tanh\left(\frac{q_e V}{2 k_\mathrm{B} T_e}\right) \tag{2.8}$$

The derivative of this function reads:

$$\frac{\mathrm{d}}{\mathrm{d}V} I_\mathrm{i} \tanh\left(\frac{q_e V}{2 k_\mathrm{B} T_e}\right) = I_\mathrm{i}\left(1 - \tanh^2\left(\frac{q_e V}{2 k_\mathrm{B} T_e}\right)\right) \frac{q_e}{2 k_\mathrm{B} T_e} \tag{2.9}$$

which can be rewritten as:

$$\frac{\mathrm{d}}{\mathrm{d}V} I_\mathrm{i} \tanh\left(\frac{q_e V}{2 k_\mathrm{B} T_e}\right) = I_\mathrm{i} \operatorname{sech}\left(\frac{q_e V}{2 k_\mathrm{B} T_e}\right) \frac{q_e}{2 k_\mathrm{B} T_e} \tag{2.10}$$

Since

$$\operatorname{sech}\left.\frac{q_e V}{2 k_\mathrm{B} T_e}\right|_{V=0} = 1 \tag{2.11}$$

the sech part in Equation 2.10 disappears in $V = 0$. Therefore, at the origin $I = 0$ and $V = 0$, the slope reads:

$$\left.\frac{\mathrm{d}I}{\mathrm{d}V}\right|_{V=0} = \frac{I_\mathrm{i} q_e}{2 k_\mathrm{B} T_e} = \frac{I_\mathrm{i}}{2 \bar{T}_e} \tag{2.12}$$

The quantities $\mathrm{d}I/\mathrm{d}V|_{V=0}$ and I_i can be estimated from a $I(V)$-curve measured using a double Langmuir probe. Then, $\bar{T}_e$ can be obtained using Equation 2.12, and n_b can subsequently be estimated from Equations 2.6 and 2.7. [1]

It should be noted that, like every other conducting surface, the tips of the probe induce the creation of a sheath. The probe tips are negative with respect to the plasma when $V = 0$. Therefore, only the high-energy tail of the electron distribution is collected by a double probe. [1] [4] It is however not known by how much the electron temperature is overestimated.

2.3 Optical Emission Spectroscopy

Assuming hydrogen excitation only occurs upon electron impact, rate coëfficients for the excitation of molecular or atomic hydrogen can be calculated. [5] Such an excited particle is marked by an asterisk*. Two different types of excitation will take place: direct excitation of a hydrogen atom by a fast electron ($H + \vec{e} \rightarrow H^* + e$) and dissociative excitation of a hydrogen molecule, leaving two hydrogen molecules, one of which is excited ($H_2 + \vec{e} \rightarrow H + H^* + e$). The excited atom will eventually fall back to a lower energy level, emitting a photon with the same energy as the difference between the energy levels before and after the transition.[5]

When the temperature distribution of the electrons is assumed Maxwellian, the rate coëfficients for the dissociation of hydrogen to the $n = 3$ and $n = 4$ levels (where n is the principal quantum number) can be calculated for both excitation processes. The transition $n = 3 \rightarrow n = 2$ results in the emission of a photon with a wavelength of 656.3 nm, while the $n = 4 \rightarrow n = 2$ transition emits a 486.1 nm photon. These are, respectively, the H_α and H_β Balmer lines.

The rate coëfficients Q [cm^3·s^{-1}] for the excitation processes that lead to the emission of these H_α and H_β lines are shown in Figure 2.1, for a range of electron temperatures. [5]
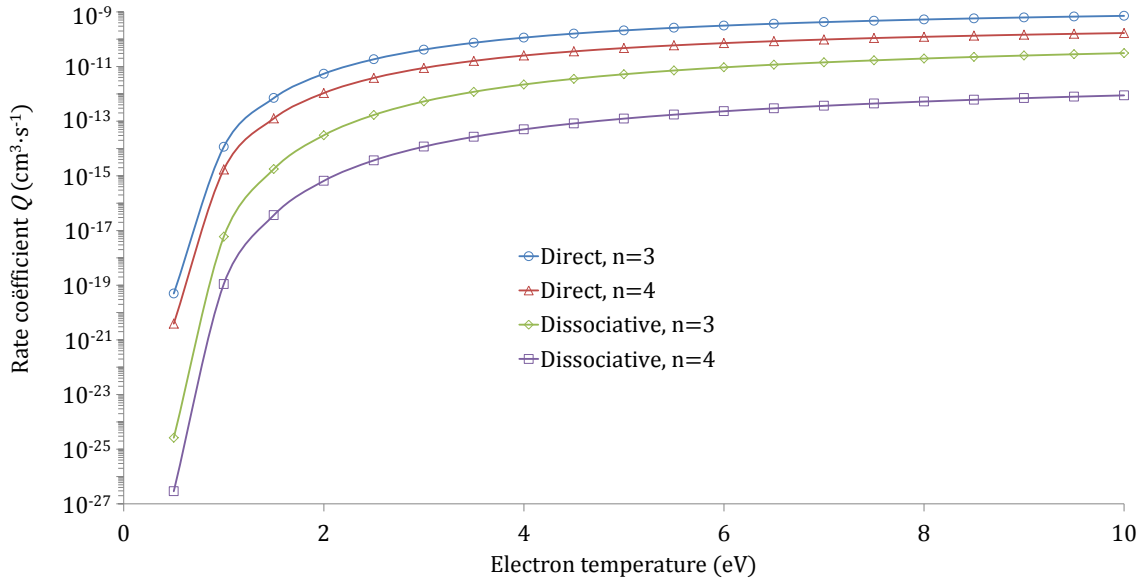

Figure 2.1: Rate coëfficients Q of direct and dissociative excitation of hydrogen to the $n = 3$ and $n = 4$ levels by electron impact as a function of the electron temperature.

For a given electron temperature (which may either be obtained by simulation or by measurement), the density ratio of atomic and molecular hydrogen is calculated from the following relation: [6]

$$\frac{I_{H\alpha}}{I_{H\beta}} = \frac{\lambda_\beta}{\lambda_\alpha} \frac{\left(kQ_{\text{direct},n=3} + Q_{\text{dissociative},n=3}\right)}{\left(kQ_{\text{direct},n=4} + Q_{\text{dissociative},n=4}\right)} \tag{2.13}$$

Here, $I_{H\alpha}$ and $I_{H\beta}$ are the intensities of the H_α and H_β spectral lines, λ_α and λ_β are the wavelengths of these lines, Q is the rate coëfficient for each of the four excitations, and k is the

density ratio of atomic and molecular and molecular hydrogen:

$$k = \frac{n_{\mathrm{H}}}{n_{\mathrm{H}_2}} \tag{2.14}$$

When the H_α and H_β intensities are measured and the electron temperature is known, the density ratio of atomic and molecular hydrogen is calculated from Equation 2.13. Alternatively, the dissociation degree, the fraction atomic particles of the total amount of neutral particles, can be calculated:

$$a = \frac{k}{k+1} \tag{2.15}$$

where a is the dissociation degree and k is the density ratio. Combining Equations 2.13 and 2.15 and the data presented in Figure 2.1 results in a relation between the line intensity ratio and the dissociation degree. This relation is shown in Figure 2.2 for three electron temperatures. For a measured electron temperature and line ratio, the dissociation degree is determined in this way. Around the measured degree of dissociation, these values are calculated in a 0.1% interval.
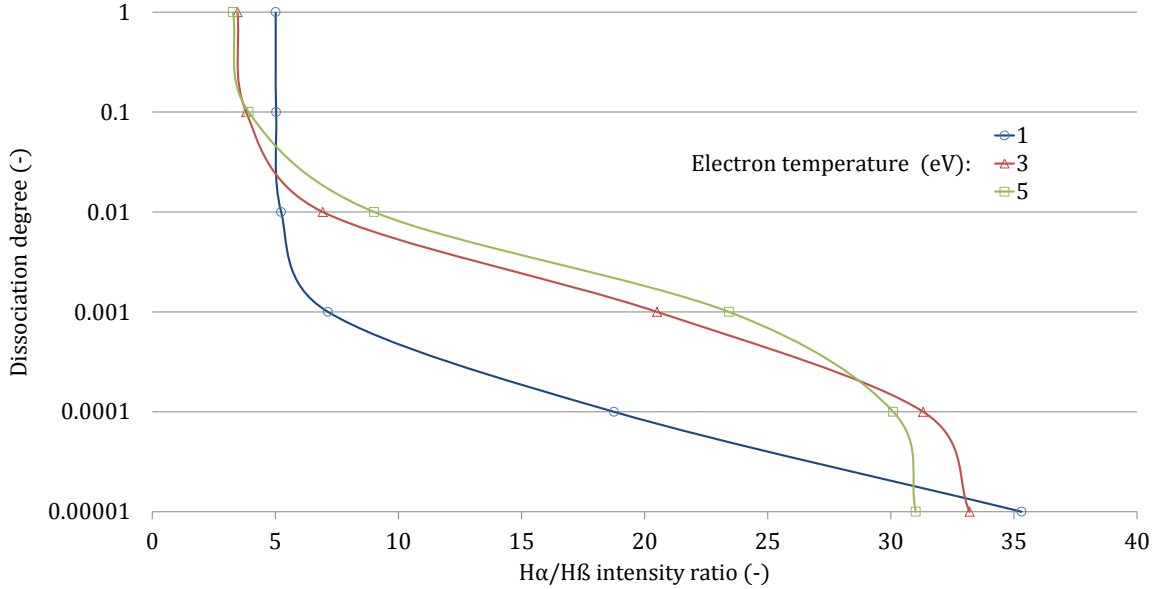

Figure 2.2: Dissociation degree as a function of hydrogen line intensity ratio for three electron temperatures.

2.4   Catalytic Probe

Two-body diatomic hydrogen recombination ($H + H \rightarrow H_2$) cannot occur in a plasma because of conservation of energy and impulse. Diatomic hydrogen recombination in a plasma therefore relies on three-body interactions, e.g. $H + H + H \rightarrow H_2 + H$, where the hydrogen atom carries away the recombination energy. However, when a hydrogen atom arrives at a surface and sticks to it, it may recombine with another hydrogen atom, releasing the recombination energy to the surface in the form of heat. This process can be utilized to measure the arriving flux of atomic

hydrogen on a probe surface:

$$\phi_H = \frac{2 N_A \dot{Q}_{\text{rec}}}{A \gamma \Delta H_{\text{rec}}} \quad (2.16)$$

Where ϕ_H (m^{-2}·s^{-1}) is the atomic hydrogen flux, $N_A = 6.02 \cdot 10^{-23}$ (mol^{-1}) is Avogadro's constant, $\dot{Q}_{\text{rec}}$ (W) is the measured heat load on the sensor, A (m^2) is the probe area, γ (-) is the recombination coëfficient (i.e., the chance a hydrogen atom will recombine before leaving the surface) and $\Delta H_{\text{rec}} = 435.94$ (kJ·mol^{-1}) is the recombination heat. The factor of 2 is there because two hydrogen atoms are needed to form one hydrogen molecule.

For some metals, for instance Platinum, $\gamma \approx 1$ under most circumstances. [6] A probe may be created from a thermocouple made of such a material or by attaching a thermocouple to a metal sheet. The recombination heat load can be calculated using a heat balance model of the probe. The various heat flows are shown in Figure 2.3.
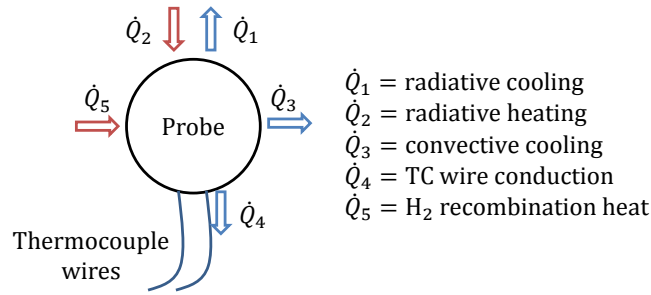

Figure 2.3: Schematic representation of heat flows at probe surface.

When the probe temperature is stable, the hydrogen recombination heat load can be written as:

$$\dot{Q}_{\text{rec}} = \dot{Q}_5 = \dot{Q}_1 + \dot{Q}_3 + \dot{Q}_4 - \dot{Q}_2 \quad (2.17)$$

When the temperature dependence of $\dot{Q}_1$, $\dot{Q}_2$, $\dot{Q}_3$ and $\dot{Q}_4$ are known (either by measurement or by calculation using a model), the recombination heat load is calculated from the probe temperature. Then, the hydrogen radical flux at the probe surface can be calculated from $\dot{Q}_{\text{rec}}$ using Equation 2.16. [6]

Alternatively, a second probe of the same dimensions may be built with $\gamma \approx 0$ (for instance, a thermocouple covered in quartz) and a heater such as a resistor embedded in the probe. Now, the electrical energy needed to keep this second probe at the same temperature as the first probe equals the recombination heat load on the first probe. [7]

While this is a suitable method for the determination of hydrogen radical densities, the application of this method is beyond the scope of this study.

Chapter 3

Plasma Setup & Diagnostics Methods

3.1 RF Plasma Setup

The setup used for the experimental part of this study is concentrated around a sapphire (crystalline Al_2O_3) tube with an inner radius of 2 cm. A gas is let into the system while it is evacuated. Electrical power with an RF frequency of 13.56 MHz is inductively coupled into the gas using a 5-turn copper coil. An electrical matching network continuously compensates for the change of coil inductance in order to minimize the power reflected by the plasma, so maximum RF power is absorbed by the plasma. From the gas inlet side of the tube, probes or sample holders may be inserted into the tube for measurements or exposures. Figure 3.1(a) shows a schematic drawing of the setup.

As is visible in Figure 3.1(b), a grounded shielding array of copper strips is wrapped around the tube. These strips shield the plasma from the capacitive part of the RF signal, i.e., the voltage across the length of the coil. This capacitive potential difference accellerates ions to high velocities (resulting in etching of the tube and the sample) and therefore has to be suppressed.

The RF source power level is set to any value up to 325 W. Under normal circumstances, the reflected power is zero so the actual plasma power is equal to the selected power. However, when the maximum of 325 W is selected, the forward power of the RF source is not entirely stable and never exceeds 319 W. Therefore, for this study a maximum RF power of 300 W is chosen. Depending on gas pressure, the minimum power that can maintain a plasma lies between 150 W and 300 W.

The pump speed can manually be adjusted using an adjustable gate valve. The hydrogen flow is controlled either manually by a needle valve, or computer controlled to keep the system at constant pressure. The hydrogen flow rate is measured by a mass flow controller.

With inductively coupled plasma setups, it is usually hard to ignite the plasma because the electric fields in the gas are not sufficiently large to initially ionize molecules. On this particular setup, a tesla gun is used to introduce free electrons to the gas. Accellerated by the RF, these electrons ignite the plasma, which can then be maintained by the RF system.

3.2 Double Langmuir Probe

The Langmuir probe used for this study is shown schematically in Figure 3.2. The tips have a 2.5 mm-diameter and are 14 mm apart (center to center). Two probe tip thicknesses were used: 0.10 mm and 1.0 mm, resulting in total probe areas of 5.7 and 13 mm^2, respectively. Using the linear manipulator, the probe can be positioned at any distance from the coil between 0 mm and 90 mm. This is the distance of the probe tips to the last turn of the coil. All of the
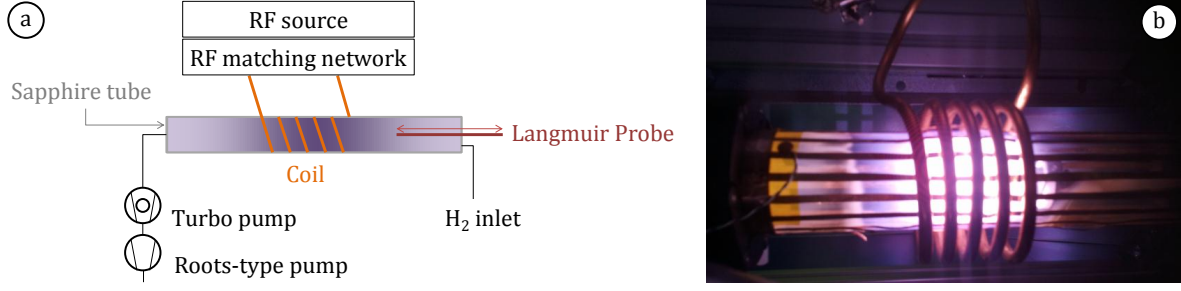
Figure 3.1: (a) Schematic drawing of the RF plasma setup, and (b) photo of the tube with coil, shielding and plasma glow visible.

probe measurements presented are performed at one or more of the following distances: 10 mm, 30 mm, 50 mm, 70 mm, 90 mm. In any case, the probe is located at the center of the tube, radially. No attempt are made to measure any radial gradients in the plasma.

The probe is attached to a Keithely 6517B electrometer, which is used to sweep the probe bias from -30 V to +30 V and measure the probe current at the same time. The electrometer is connected to a computer, both to control the bias voltage and to log the measured current. Between the probe and the electrometer, an electronic notch filter prevents the 13.56 MHz RF-signal to be transmitted to the electrometer.

An example of the $I(V)$-curve from a double Langmuir probe measurement is shown in Figure 3.3, marked by the blue circles. Note that, as opposed to the theoretical prediction, the ion current is not limited but slowly keeps rising with the voltage. This is a linear effect due to the sheath at the probe surface. The thickness of this sheath increases with the voltage applied to it, thereby increasing the effective probe area. One can easily correct for this by substracting a line with the same slope as the ion currents from the entire measurement, also shown in Figure 3.3 by the red triangles. The slope at $V = 0$, $I = 0$ is marked by the dashed red line, while the tangents to the curve to obtain the ion currents I_{1i} and I_{2i} in $V = 0$ are marked by the dotted green lines. The ion currents I_{1i} and I_{2i} for probe voltages $V < 0$ and $V > 0$, respectively, are averaged to obtain the net ion current I_i.

An alternative method for the analysis of the obtained $I(V)$-curve is by fitting a tanh-curve of the form of Eq. 2.8 to a corrected measurement. For the analysis of one measured $I(V)$-curve both methods were used, yielding the same results.
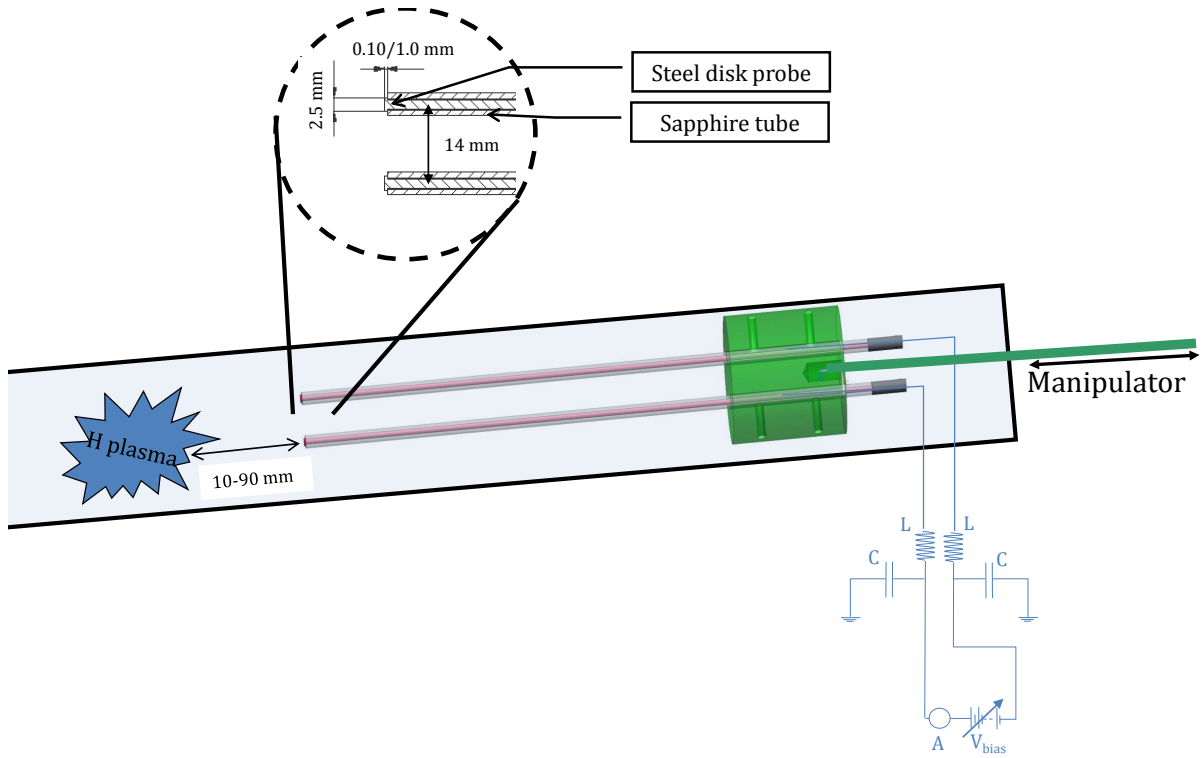
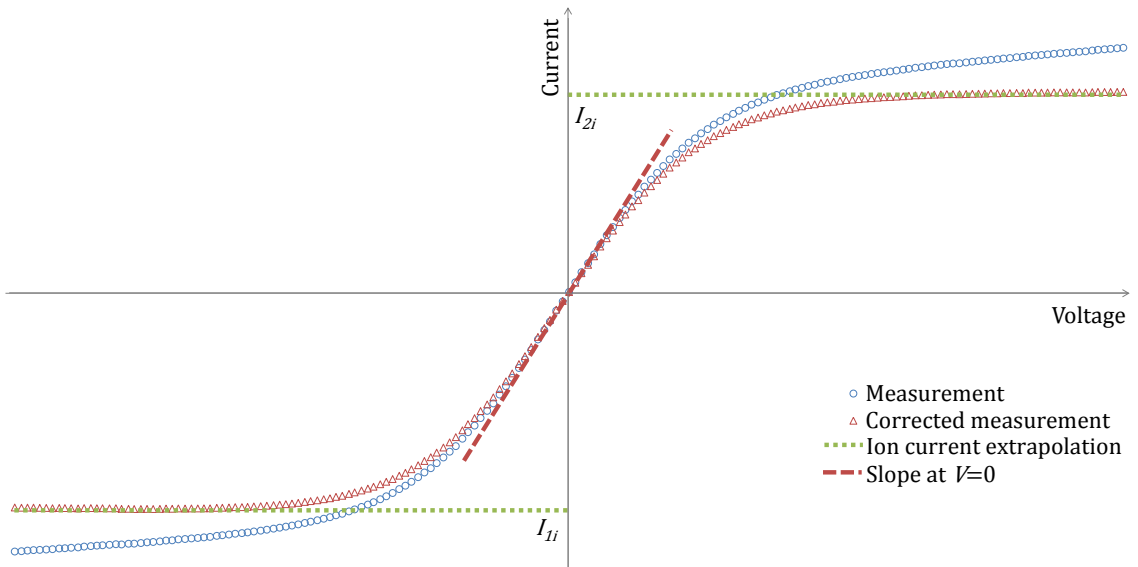Figure 3.2: Schematic drawing of the double Langmuir probe, including the electronic filter network.

Figure 3.3: Example of a $I(V)$-characteristic as measured by a double Langmuir probe and $I(V)$-curve corrected for sheath expansion. The dotted green lines represent the way in which the ion currents I_{1i} and I_{2i} are determined; these are then averaged to obtain I_i. The dashed red line represents the slope of the $I(V)$-curve at $V = 0$, $I = 0$.

3.3 Spectrometer

For the spectrometric measurements, an Ocean Optics USB2000+ spectrometer is used. The end of the fiber connected to the spectrometer was positioned just outside the sapphire tube, at the center of the discharge (between two turns of the coil). Accurate local measurements outside the coil region are not possible, due to reflections on the inside of the tube; in the coil region, this is not a problem. A sample spectrum of the plasma is shown in Figure 3.4, already corrected for background (ambient light) and the CCD's dark current. The H_α and H_β lines are clearly visible at 656 nm and 486 nm, respectively. The broad peak around 600 nm is the Fulcher-α band, originating from molecular hydrogen transitions. Also, there seems to be a continuous spectrum from low wavelength up to around 650 nm. The origin of this part of the spectrum is unknown, but is thought to come from luminescence of the sapphire tube.

The spectrometer was connected to a halogen calibration lamp in order to measure the spectral response of the spectrometer. This is the combined response of the individual optical fiber, grating and CCD responses. This method is shown in Appendix A, resulting in an additional factor of 1.23, with which the measured $\frac{H_\alpha}{H_\beta}$ ratio should be multiplied.

For each measurement, the peak intensity is calculated as the total photon count along the line width, while the background level of the continuous spectrum (the average signal between 500 and 550 nm) is substracted. The ratio of the line intensities is subsequently used to determine the dissociation degree using the data presented in Figure 2.2, with the appropriate electron temperature selected as measured using the Langmuir probe. This method is shown in Figure 3.5, with an electron temperature of (3.5±0.5) eV and $\frac{H_\alpha}{H_\beta}$ line intensity ratio of 7.0 ± 2%. In this example, the dissociation degree is $(0.014^{+0.009}_{-0.006})$ or $(1.4^{+0.9}_{-0.6})\%$.
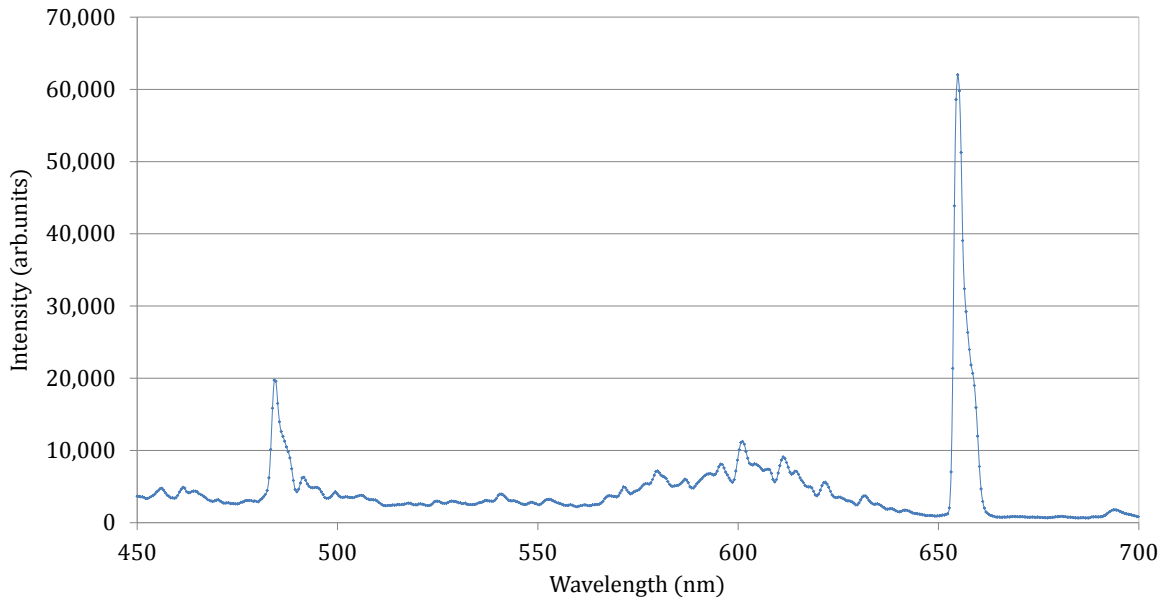

Figure 3.4: Example of spectrum of the hydrogen plasma, measured by the spectrometer, corrected for the black spectrum.
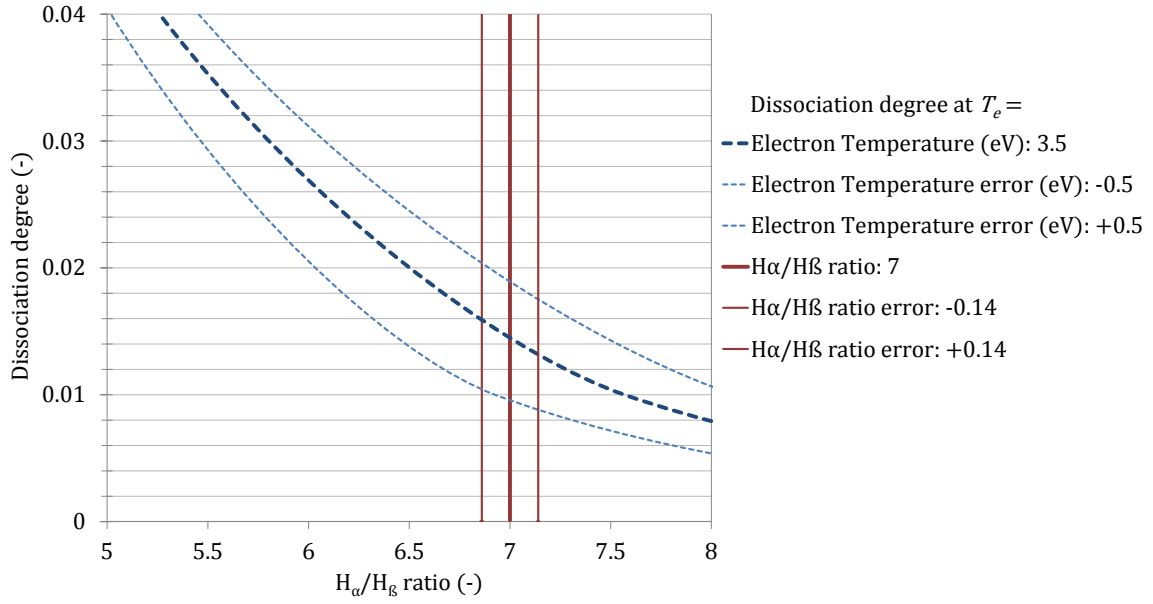
14

Figure 3.5: Example of the determination of the dissociation degree, combining $\frac{H_\alpha}{H_\beta}$ line intensity ratio and measured electron temperature.

3.4 Error Analysis

3.4.1 Langmuir Probe

Several possible causes for uncertainty in these measurements can be noted:

- Plasma disturbance by the bias voltage. Since the plasma shields itself from electric fields at length scales larger than the Debye length (typically 0.01 - 0.1 nm for this type of plasma), there are no effects other than the sheath expansion, which is already corrected for. [1]

- Geometry of the probe tips. An ideal probe tip is a flat surface facing towards the plasma. [1] The probe used for this study has cylindrical tips. However, when tips with different thickness are used (0.1 and 1.0 mm, respectively) and the entire surface is used in the calculations, the measurements yield the same results.

- Small position difference between probes. When one probe sticks out a bit further into the plasma, the plasma parameters will differ between the two tip positions. A position difference of more than 0.5 mm would easily be noticed by eye. A measurement with a position difference of 2 mm was taken to determine the effect on the measured $I(V)$-curve and the calculations. A difference in electron temperature (4%) and plasma density (8%) was measured compared to a probe with two well-aligned tips.

- Due to gravity acting downwards on the probe, the two probe tips are not always at the same distance from the center of the tube, radially. When the probe holder is rotated while $V = 0$, the current fluctuates. The probe is assumed to be centered when $I(0) = 0$. Measurements were taken for $I(0) = 0$, $I(0) = $ maximum (negatively) and $I(0) = $ maximum (positively). The $I(V)$-curve for $I(0) = 0$ is symmetric, the other two curves

asymmetric. This results in maximum differences in electron temperature and plasma density of 12% and 28%, respectively.

- Contamination (e.g., a thin oxide layer) on the probe surface. To verify the effect, one of the tips of a used probe was cleaned abrasively. The measured $I(V)$-curve is somewhat higher at the side of the cleaned tip (indicating contamination on the uncleaned tip surface), but both the ion current extrapolation and the slope at $V = 0$ are similar to a measurement with two uncleaned probe tips. Moreover, the slope of the curve at the origin does not change. Since a contamination layer effectively acts as a resistance, it will have a effect on the current that is linear with the bias voltage. Since the compensation for sheath expansion removes any linear components from the $I(V)$-curve, the presence of a small contamination layer will have no influence on the measurement results.

To determine the total error caused by these uncertainties, six probe measurements were taken at 10 mm, 60 sccm H_2 flow and 8 Pa background pressure:

- 1mm thick probe, normal settings

- 1mm thick probe, probe tip position difference of 2 mm

- 1mm thick probe, one tip cleaned

- 0.1mm thick probe, $I(0) = 0$

- 0.1mm thick probe, $I(0) = \max$ (negatively)

- 0.1mm thick probe, $I(0) = \max$ (positively)

From these measurements, the average electron temperature and plasma density was calculated, as well as the standard deviation σ. This is shown in Appendix A. An error of 2σ will be used: for $\bar{T}_e$, the error is 13%, while for n, the error is 29%.

3.4.2 Spectrometer

The spectrometer used for this study is an Ocean Optics USB2000+. Sources of error in the $\frac{H_\alpha}{H_\beta}$ ratio may be:

- The optical resolution of the spectrometer. The USB2000+ has a 25 μm-slit installed, and Grating 31 with a wavelangth range of 200 to 1050 nm. The optical resolution (nm) is defined as: [8] Optical Resolution = Dispersion · Pixel Resolution. The dispersion (nm·pixel^{-1}) is given by: Dispersion = Spectral Range of the Grating / Number of Detector Elements $= \frac{1050-200}{2048} = 0.42$ nm·pixel^{-1}. The pixel resolution for this device/slit-combination is 4.2 pixels. The optical resolution is therefore $0.42 \cdot 4.2 = 1.8$ nm, which is adequate for this purpose because the hydrogen spectrum is well known, and the spectral lines of interest are not close to any other spectral lines since hydrogen is the only gas in the system. The narrow hydrogen lines will be broadened (this is indeed observed), so the sum of the counts in the peak will be used as measure for the peak intensity.

- Dark current of the CCD sensor. During each measurement session, a black spectrum was taken, and substracted from each measurement. The dark current of the spectrometer is constant over time and does not vary with integration time. Therefore, dark current is assumed not to be a source for any error. The dark noise of the CCD is specified by the manufacturer as 50 counts RMS. [9] When added to the emission line integrals of the

measurements, this noise generates an error of 0.2% for the H_α line and 0.5-0.8% for the H_β line.

- The spectral response of the spectrometer; the spectral response was calibrated using a halogen calibration lamp, as described in Appendix B. Any remaining error due to the spectral response differences are neglected.

- Linearity of the sensor; this is specified by the manufacturer as 99%, leaving an uncertainty of 1%. [9]

- The 'continuous spectrum' around the H_β line. The average signal between 500 and 550 nm is substracted from the peak area to compensate for the increased signal level. The standard deviation of the signal between 500 and 550 nm is used to calculate the uncertainty in the H_β line. This leads to an uncertainty between 4% and 10%.

- The position of the fiber relative to the plasma. Only the bulk of the plasma is studied, and the plasma is assumed to be uniform in the region inside the coil. [1] Therefore, no variations are expected as long as the fiber is pointed directly at the plasma bulk region.

From these uncertainties, the total $\frac{H_\alpha}{H_\beta}$ ratio uncertainty is calculated for each spectrum. This value varies between 5% and 11%.

Chapter 4

Plasma Measurements - Results and Discussion

In this chapter, results of the double Langmuir probe measurements and optical emission spectroscopy will be presented and discussed.

4.1 Plasma Dependence on RF Power

The most direct way to alter plasma properties is to change the output of the plasma power source. Changing the power will result in a change in the plasma properties that are relevant to the environment at the test sample location.

When $\bar{T}_e$ is calculated assuming particle conservation in a uniform density discharge, it follows that $\bar{T}_e$ is independent of the plasma density and therefore input power. In a steady state however, this power has to be dissipated to the vessel walls, therefore the plasma density must be dependent on power.[1]

Double Langmuir probe measurements were taken with the RF source operating at different power levels: 150 W, 200 W, 250 W and 300 W (at higher pressures, the minimum power required to maintain the plasma increases). These measurements were taken at five different positions relative to the last coil, i.e. 10 mm, 30 mm, 50 mm, 70 mm and 90 mm. The results are presented in Figures 4.1 and 4.2, showing electron temperatures and plasma densities, respectively.

Electron temperatures rise by less than 0.5 eV when the power is increased from 150 W to 300 W. This result is roughly in accordance to the theory which predicts that the electron temperature is not a function of the input power. The density, on the other hand, depends linearly on plasma power. At different positions, the relative changes in density are comparable. This shows that already at low power, there is a balance between the heating of electrons by the power source and the transfer of energy from electrons to other species, again resulting in the creation of ion-electron pairs. When this balance point is reached, additional power will mainly result in creating more ions and electrons, while the energy of these species is not allowed to rise significantly.

The degree of dissociation was measured for three different power settings at 20 Pa, 20 sccm. The results, shown in Figure 4.3, are inconclusive as to the power dependency of the hydrogen atom density.
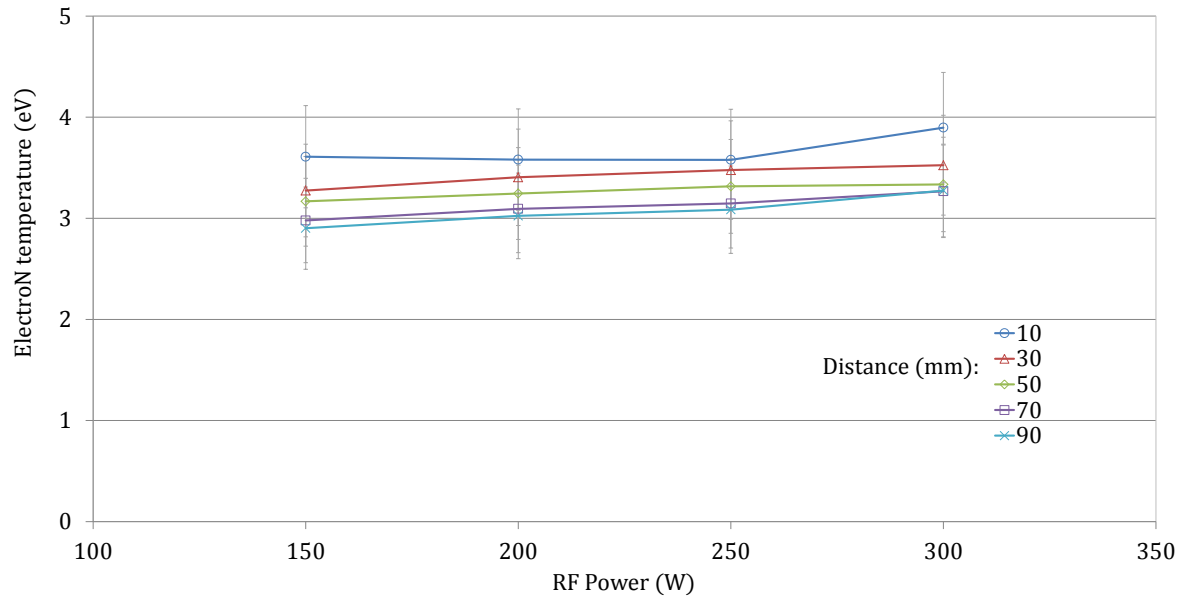
Figure 4.1: Electron Temperature as a function of RF power at five different positions, H_2 pressure $p = 5$ Pa. Electron temperatures increase by less than 0.5 eV when RF power is increased from 150 W to 300 W.
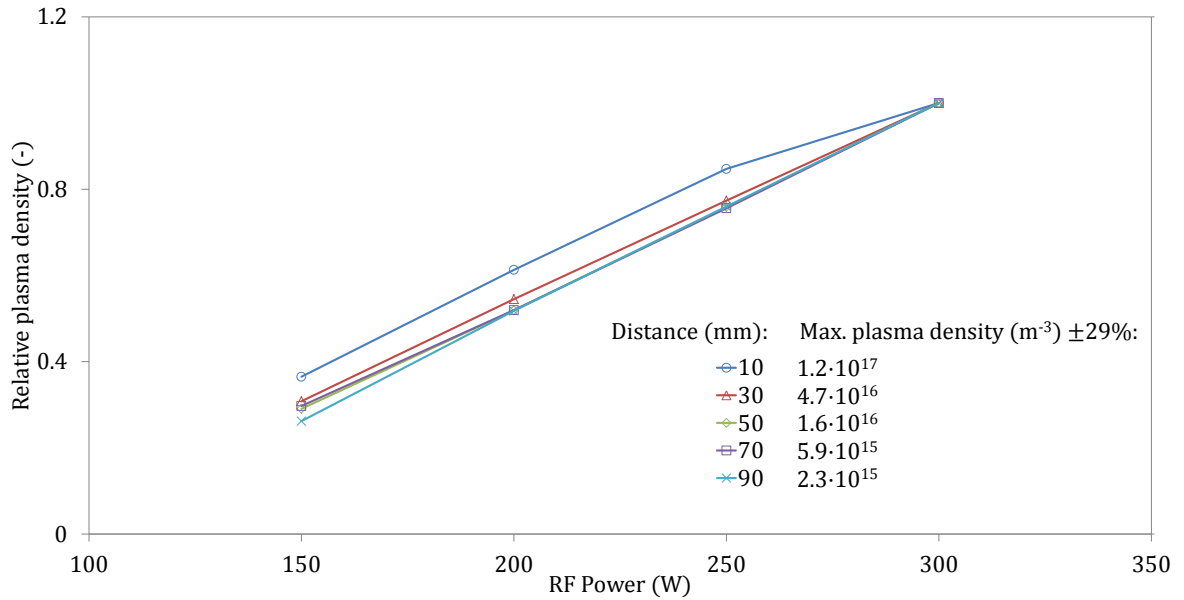

Figure 4.2: Relative plasma density (the fraction of the density at 300 W) as a function of RF power at five different positions, H_2 pressure $p = 5$ Pa. Density at 300 W is also listed. Throughout the distance range, plasma density is linear with RF Power.
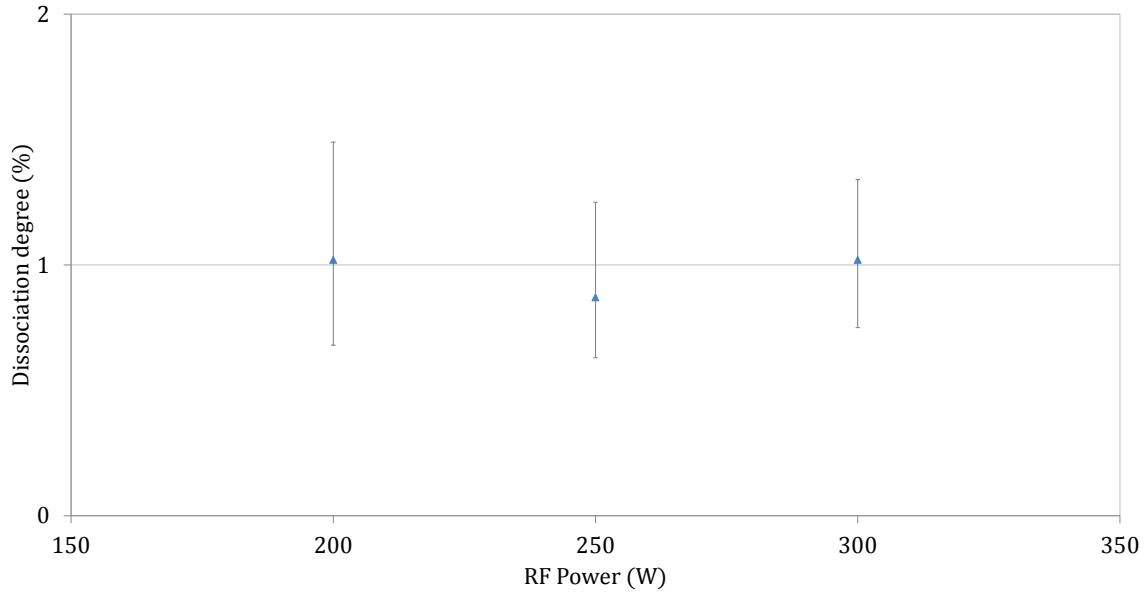
Figure 4.3: Degree of dissociation of the hydrogen gas as a function of RF power at 20 Pa and 20 sccm.

4.2 Plasma Dependence on H_2 Pressure

The gas pressure or neutral gas density is an important parameter in plasma formation and propagation. Since all RF power is absorbed by only the electrons, the presence of all particles beside neutral gas molecules and electrons is the result of interactions between all species. Since the neutral gas density is several orders of magnitude larger than the plasma density ($n \approx 10^{14} - 10^{18}$ m^{-3}, $n_g \approx 10^{21} - 10^{22}$ m^{-3} between 5 Pa and 35 Pa), most collisions of charged particles are with neutral atoms or molecules. A change in neutral gas density will change the distance between most collisions, which results in a shift in particle balance.

The electron temperature and plasma density was measured at two distances to the coil for a range of pressure settings. The results are shown in Figure 4.4. At both distances, the electron temperature is maximum at low pressure, and decreases by 1 eV when the pressure is increased to 35 Pa. The difference in $\bar{T}_e$ between 10 mm and 90 mm varies between 0.5 and 1 eV. At 10 mm, the density is independent of hydrogen pressure. As this position is still in the plasma creation region, the plasma composition is unaffected by diffusion processes. At 90 mm, it is clear that diffusion losses play a large role, decreasing the density by one order of magnitude when pressure is increased from 5 Pa to 35 Pa.

The dissociation degree was measured at a hydrogen flow rate of 20 sccm and RF power of 300 W. The dissociation degree between 5 Pa and 35 Pa is shown in Figure 4.5. Multiplied by the pressure-dependent neutral gas density, the degree of dissociation results in a value for the density of atomic hydrogen n_H (m^{-3}) as shown in Figure 4.6. When the pressure is increased, the atomic hydrogen density also increases, but not linearly since the dissociation degree decreases with increasing pressure.
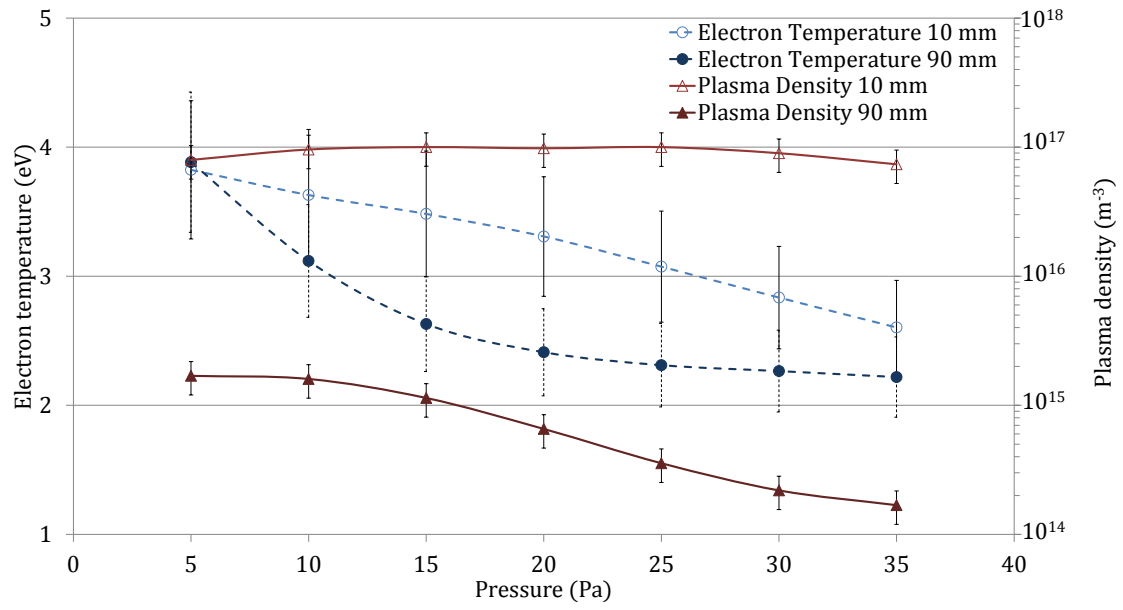
Figure 4.4: Electron temperature and plasma density between 5 Pa and 35 Pa at 10 mm and 90 mm away from the coil. RF Power is fixed at 300 W.
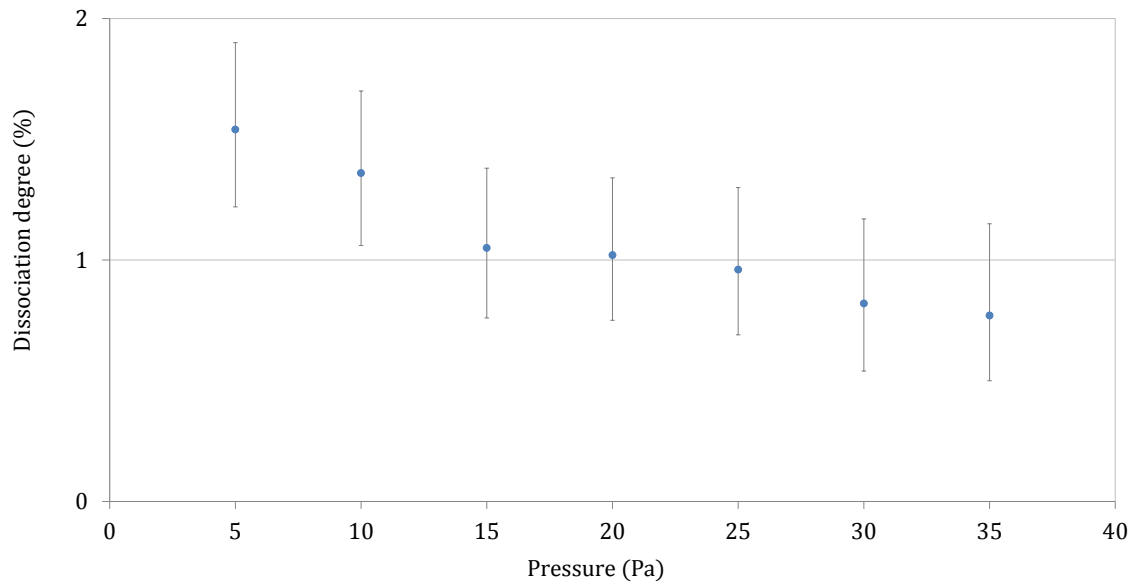

Figure 4.5: Degree of dissociation of the hydrogen gas as a function of background pressure.
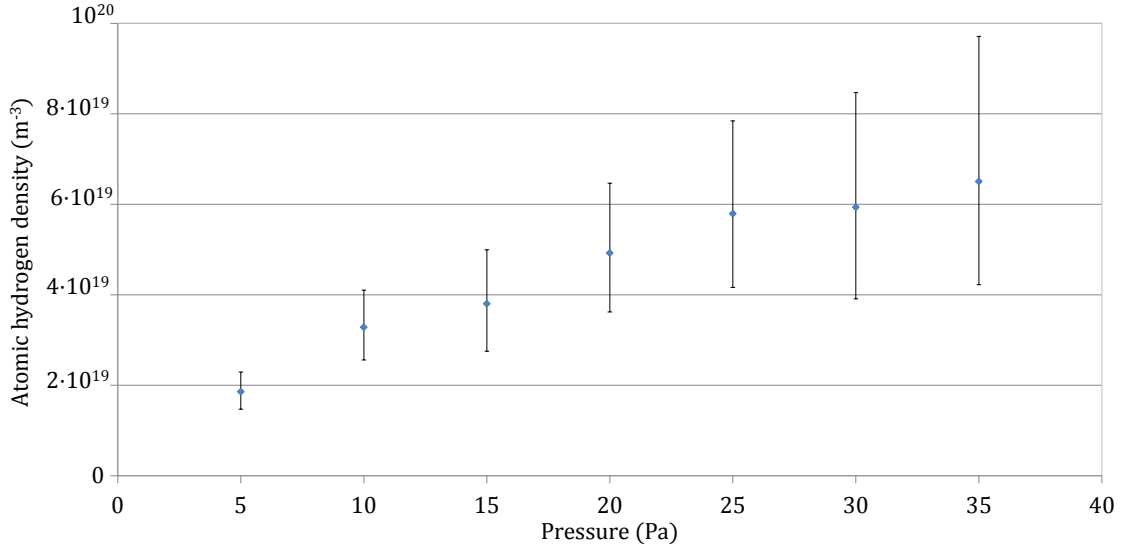
Figure 4.6: Atomic hydrogen density inside the discharge, for 20 sccm and 300 W.

4.3 Plasma Dependence on H_2 Flow

The gas pressure is an important parameter in the plasma creation and expansion processes. In laboratory conditions, this gas pressure is the result of gas inflow at one point, and a pumping system at another point in the system. In this section, experiments will be shown to determine plasma formation and plasma expansion dependencies on hydrogen flow rate.

A series of measurements was performed during which the H_2 flow and pressure were controlled independently. At three hydrogen flow rates, three pressures were chosen. Langmuir probe measurements at two positions, 10 mm and 90 mm, were taken. The resulting electron temperatures and plasma densities, respectively, are shown in Figures 4.7 and 4.8. The electron temperature as well as the plasma density is, at both distances and all pressure settings, independent of the hydrogen flow rate.

Using the spectrometric method, the dissociation degree was determined at constant pressure, constant RF power. In Figure 4.9 the results are shown, indicating that the hydrogen atom density does not depend on the hydrogen flow.
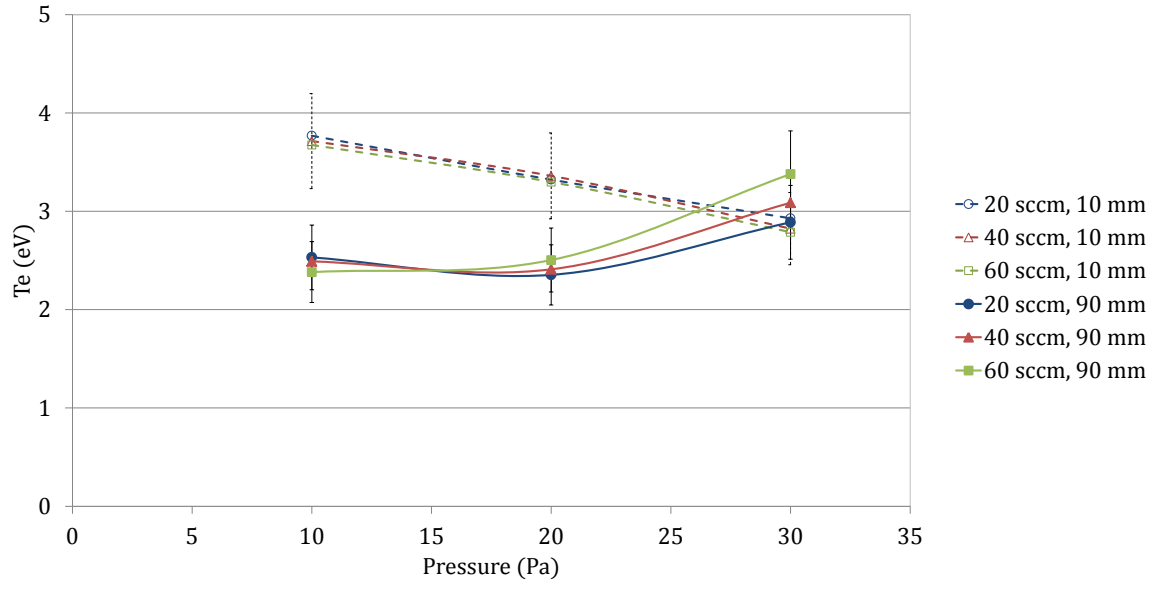
Figure 4.7: Electron temperature as a function of H_2 pressure, for three H_2 flow rates, at two distances. RF Power $= 300$ W. T_e does not significantly depend on the hydrogen flow.
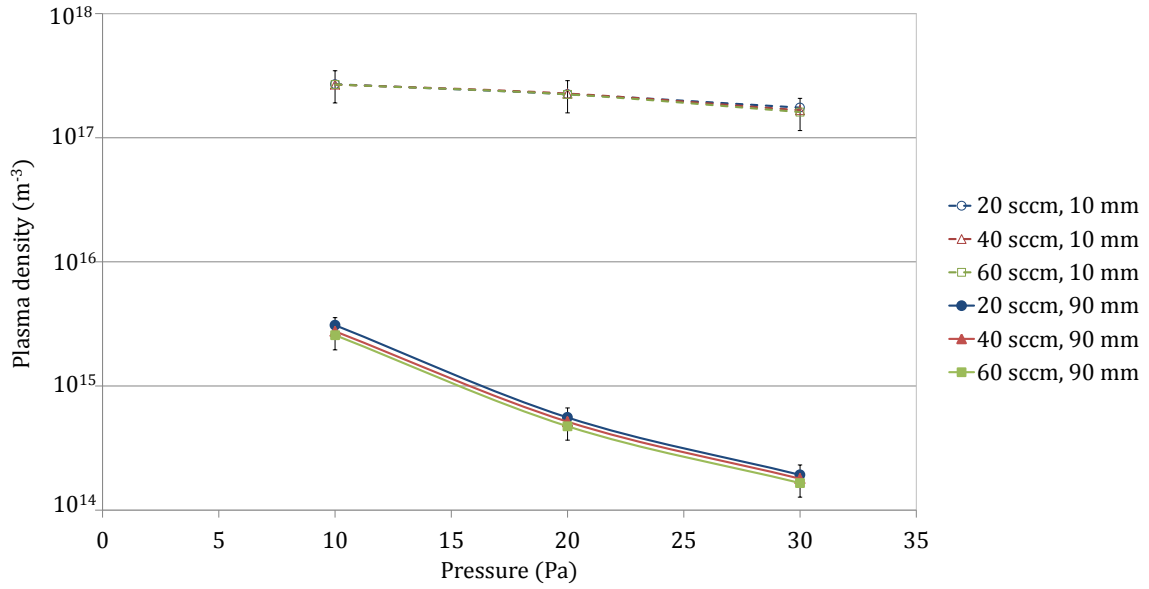

Figure 4.8: Plasma density as a function of H_2 pressure, for three H_2 flow rates, at two distances. RF Power $= 300$ W. At 10 mm distance as well as at 90 mm, plasma density does not depend on H_2 flow.
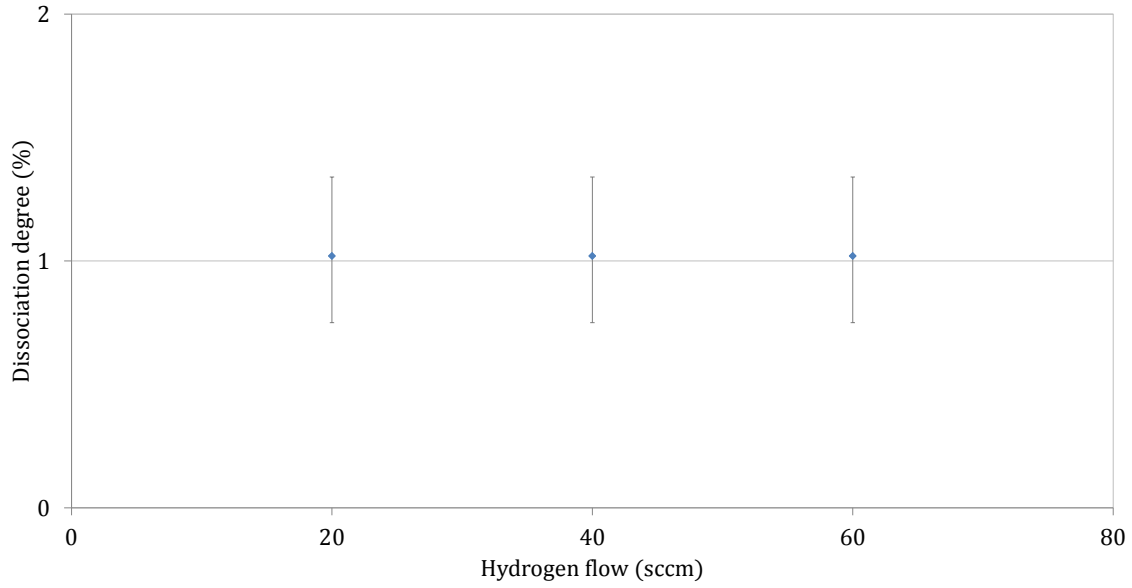
Figure 4.9: Degree of dissociation of the hydrogen gas as a function of hydrogen flow, at 20 Pa and 300 W.

4.4   Plasma Dependence on Position

Since only a part of the tube is enclosed by the RF coil, only that part of the tube is the region of active plasma creation. Any plasma outside this region will be the result of the ambipolar diffusion of electrons and ions towards both ends of the tube. In Figure 4.10, electron temperature and density are shown between 10 mm and 90 mm, while RF Power and H_2 pressure are fixed at respectively 300 W and 5.0 Pa.

Moving away from the coil, the electron temperature drops by about 1 eV, corresponding to the results shown in Figure 4.4. The measured plasma density decreases exponentially with increasing distance to the coil. This effect shows that no significant amount of plasma is being created outside the coil; since recombination of charged plasma particles is proportional to the presence of these particles, an exponential decrease would be expected, as has been shown in section 2.1.3.

Using Equations 2.4 and 2.5, the mean free path and cross section for the recombination between an electron and an ion in neutral H_2-gas can be calculated. The neutral gas density is calculated using the ideal gas law:

$$\frac{n}{v} = \frac{p}{RT} \tag{4.1}$$

with n/v (mol·m^{-3}) is the molar gas density, p (Pa) is the background pressure, $R = 8.31$ (Pa·m^3·K^{-1}·mol^{-1}) is the gas constant and $T =$300 (K) is the gas temperature. Now, the number density of the gas n_g (m^{-3}) equals:

$$n_g = \frac{n}{v} \cdot N_A \tag{4.2}$$

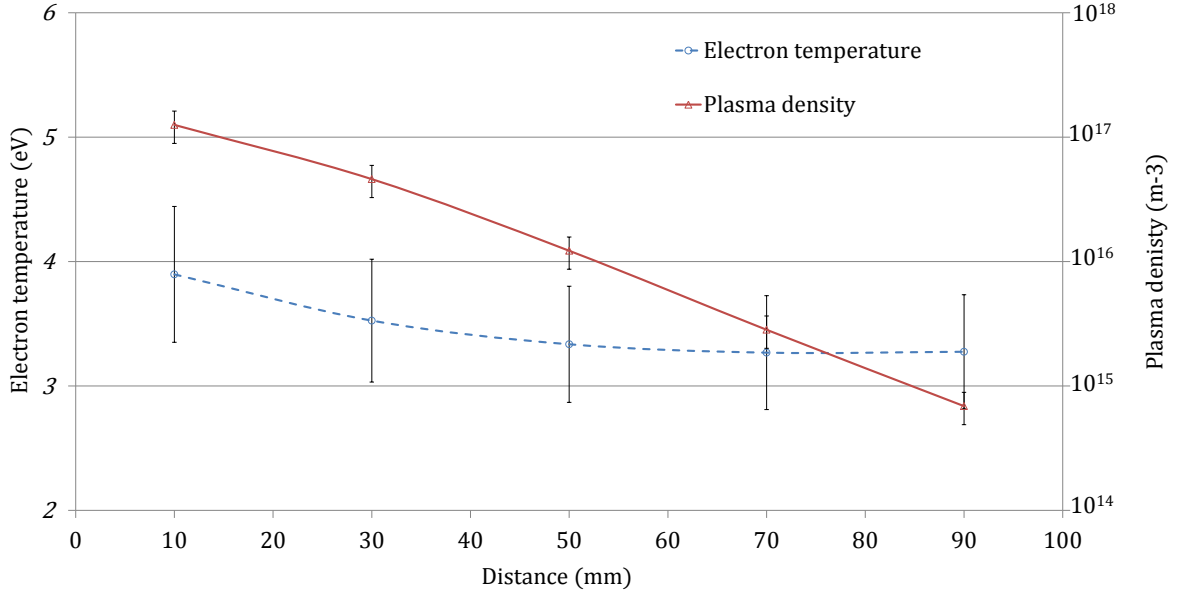where $N_A = 6.02 \cdot 10^{23}$ (mol^{-1}) is Avogadro's constant.

Figure 4.10: Electron temperature (left axis) and plasma density (right axis) as a function of distance from the last coil. RF Power = 300 W, H_2 pressure = 5.0 Pa.

The resulting figures for the recombination mean free path $\lambda_{\rm rec}$ (mm) and cross section $\sigma_{\rm rec}$ (mm^2) at various pressures are listed in Table 4.1. The mean free path is the distance across which the plasma density decreases to a fraction of the original density of $(1 - {\rm e}^{-1}) \approx 0.63$ in a neutral H_2-gas, and the cross section is the average of the effective cross sections for the various recombination processes, for instance $H^+ + e^- \rightarrow H$, $H_2^+ + e^- \rightarrow H_2$, $H_3^+ + e^- \rightarrow H_2 + H$. [2]

Since this recombination is an effect outside the RF coil, the RF power is expected to have no influence on the recombination process. Indeed, the mean free path and recombination cross section are only dependent on pressure and not on RF power.

Table 4.1: Mean free path and recombination cross section at various pressures.

p (Pa)	$\lambda_{\rm rec}$ (mm)	$\sigma_{\rm rec}$ (mm^2)$\cdot 10^{-14}$
5.0	19^{+3}_{-5}	$4.5^{+0.7}_{-1}$
15.0	14^{+2}_{-3}	$2.0^{+0.3}_{-0.4}$
20.0	13^{+2}_{-3}	$1.6^{+0.2}_{-0.3}$
35.0	12 ± 2	$1.0^{+0.1}_{-0.2}$

Chapter 5

Conclusions

5.1   Comparison with Model

At 10 mm distance, the bulk discharge charactericstics were measured. The most direct ways to influence the plasma is by changing the background pressure and the RF source power output. Additionally, the hydrogen flow rate has been varied. In this section, the results will be compared to the simulations of a 0-dimensional model of this plasma setup. [3]

When the RF power is changed, the electron temperature rises slightly but not significantly (from (3.6±0.5) eV between 150 W and 250 W to (3.9±0.5) eV at 300 W, 5.0 Pa). The plasma density depends linearly on RF power, with a maximum of $(1.2 \pm 0.4) \cdot 10^{17}$ m^{-3} at 300 W. This shows that additional power into the plasma results in a larger number of ionizations, rather than an increase in particle energy. This is partly in accordance with the simulations. The absolute values of the electron temperature and plasma density do not correspond (simulated $\bar{T}_e = 1.93$ eV, $n = 1.8 \cdot 10^{16}$ m^{-3} with $p = 5$ Pa, $P = 300$ W), but the trend of constant electron temperature and linearly dependent plasma density are similar. These trends are also expected from literature. [1] No conclusive trends regarding the degree of hydrogen dissociation could be determined, however, a linear correlation between power and dissociation degree would be expected based on the simulations.

The plasma density showed to be independent of background pressure, being constant around $(1.0^{+0.2}_{-0.4}) \cdot 10^{17}$ m^{-3} at 300 W. The electron temperature decreases linearly with increasing pressure, from (3.8±0.5) eV at 5.0 Pa to (2.6±0.4) eV at 35.0 Pa, with P=300 W. The constant plasma density is not reflected in the simulations, which show a decrease in plasma density from $1.8 \cdot 10^{16}$ m^{-3} at 5 Pa to $3.9 \cdot 10^{15}$ m^{-3} at 35 Pa. The simulated trend in electron temperature is again in accordance to the measurements, from 1.93 eV at 5 Pa to 1.34 eV at 35 Pa. Hydrogen dissociation degrees were determined between (1.5±0.4)% at 5.0 Pa and (0.8±0.4)% at 35.0 Pa. The measurement at 5.0 Pa corresponds to the simulated value of 1.5%, while the simulations at 20 and 35 Pa (0.05% and 0.01%, respectively) are significantly lower than the measurements.

The hydrogen flow rate does not have an influence on any of the measured plasma parameters. This is confirmed by the simulations. Since the velocity of the ions and electrons is much higher than the gas flow speed (2 to 3 orders of magnitude), changes in the flow rate (and thus speed) have no significant influence on the plasma processes.

At larger distances, the expansion of the plasma in a neutral gas was studied. The electron temperature decreases when moving away from the coil, by about 0.5 - 1 eV when going from 10 mm to 90 mm. The plasma density decreases exponentially with distance, and loses 2 to 3 orders of magnitude, depending on the background pressure. From the distance-dependent density, the hydrogen recombination mean free path and cross section were calculated to be between (19^{+3}_{-5}) mm, $(4.5^{+0.7}_{-1}) \cdot 10^{-14}$ mm^2 at 5.0 Pa and (12 ± 2) mm, $(1.0^{+0.1}_{-0.2}) \cdot 10^{-14}$ mm^2 at 35.0 Pa.

There are several reasons for the discrepancy between the measurements and the simulations. The model is 0-dimensional and does not compensate for the copper shielding. The influence of this shielding on the electron temperature and plasma density is not known. The model partly relies on the recombination of atomic hydrogen at the wall surface. However, no value for the recombination coefficient of atomic hydrogen on sapphire could be found in the literature. Instead, a recombination coefficient for quartz (one of three different values found) was used. Also, he electron temperature is probably an overestimation, since the double probe only measures the high-energy tail of the electron distribution. [1] [4] This brings the measured values of the electron temperature closer to the simulation values. It is however not known by how much the electron temperature is overestimated.

5.2 Outlook

While the electron temperature and plasma density have been measured thoroughly for all input parameters, the atomic hydrogen density was not determined under all circumstances. The use of an optical method on this particular setup is limited to the discharge region, because reflections on the inside of the tube are dominant outside the coil.

To find out the origin of the continuum in the hydrogen emission spectrum, more tests could be done. A first test would involve replacing the sapphire tube with a quartz (crystalline SiO_2) tube. If this significantly changes the continuum, luminescence of the sapphire tube is the most probable source.

Catalytic probes are a good method to determine atomic densities quite directly. Unfortunately, there was not enough time to apply this method during this study. Once a catalytic probe has been constructed and calibrated, it can be used under a wide variety of circumstances.

The plasma parameter that ideally also could be measured is the ion temperature T_i, or even better, the ion energy distribution function (IEDF). A mass spectrometer or retarding field analyzer could be used to measure IEDF curves.

Bibliography

[1] M. Liebermann and A. Lichtenberg, *Principles of Plasma Discharges and Materials Processing.* New York: John Wiley & Sons, Inc, 2005.

[2] R. Janev, D. Reiter, and U. Samm, "Collision processes in low-temperature hydrogen plasmas," tech. rep., Institut für Plasmaphysik, Jülich, Germany, 2003.

[3] N. Skoro, "0-dimensional plasma simulations." Private Communication, based on 'A global model for C4F8 plasmas coupling gas phase and wall surface reaction kinetics', G Kokkoris, 2008.

[4] M. Y. Naz, A. Ghaffar, N. U. Rehman, M. Azam, S. Shukrullah, A. Qayyum, and M. Zakaullah, "Symmetric and asymmetric double langmuir probes characterization of radio frequency inductivley coupled nitrogen plasma," *Progress In Electromagnetics Research*, vol. 115, pp. 207–221, 2011.

[5] B. Lavrov and A. Pipa, "Account of the fine structure of hydrogen atom levels in the effective emission cross sections of balmer lines excited by electron impact in gases and plasma," *Optics and Spectroscopy*, vol. 92, no. 5, pp. 647–657, 2002.

[6] V. Schulz-von der Gathen and H. Döbele, "Critical comparison of emission spectroscopic determination of dissociation in hydrogen rf discharges," *Plasma Chemistry and Plasma Processing*, vol. 16, no. 4, pp. 461–486, 1996.

[7] M. R. Carruth Jr., R. F. DeHaye, J. K. Norwood, and A. F. Whitaker, "Method for determination of neutral atomic oxygen flux," *Review of Scientific Instruments*, vol. 61, no. 4, pp. 1211–1216, 1990.

[8] Ocean Optics website, "Optical resolution."
http://www.oceanoptics.com/technical/opticalresolution.asp, Nov. 2012.

[9] Ocean Optics website, "Usb2000+ product sheet."
http://www.oceanoptics.com/productsheets/usb2000+_product_sheet.pdf, Nov. 2012.

Appendix A

Double Langmuir Probe Error

As described in the error analysis, there are several causes for uncertainty in the double Langmuir probe measurements. A series of measurements was taken in which the most important variations are covered: two probe thicknesses, distance difference between the two probe tips, a cleaned probe tip and the probe rotated to achieve the most extreme current offsets in $V = 0$. The average (arithmatic mean) of the electron temperature and plasma density from these measurements was calculated, as well as the standard deviation σ:

$$\sigma = \sqrt{\frac{1}{N} \sum_{i=1}^{N} (x_i - \mu)^2} \tag{A.1}$$

where N is the number of measurements, x_i is the electron temperature or plasma density of the i-th measurement and μ is the average value of the measurements. For the electron temperature, $\sigma = 6.4\%$, while for the plasma density $\sigma = 14.5\%$. An error of 2σ (95% confidence) will be used for the results: 13% and 29% for $\bar{T}_e$ and n, respectively. The measurements, including μ and 2σ, are shown in Figure A.1.
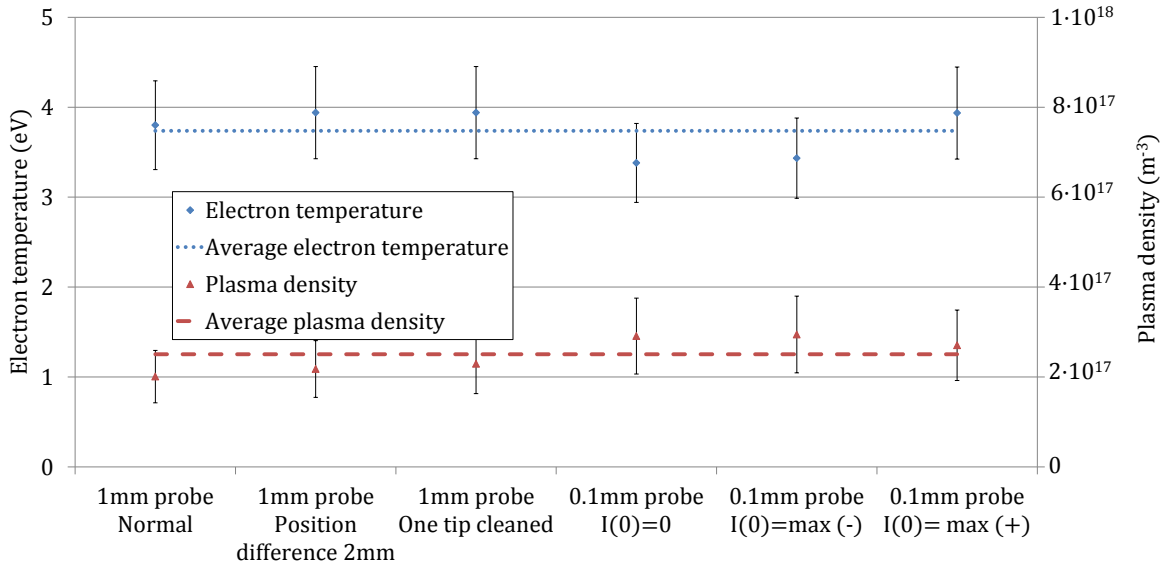

Figure A.1: Six double Langmuir probe measurements compared. Plasma parameters were equal (300 W, 8 Pa, 60 sccm H_2 flow, 10 mm distance). Average values for electron temperature and plasma density are included, as well as error bars the size of twice the standard deviation.

Appendix B

Spectrometer Calibration

The Ocean Optics USB2000+ spectrometer was calibrated using a halogen calibration lamp. The spectrum of this lamp, measured by the spectrometer, was compared to a calibration report of this lamp. By dividing the measured spectrum by the calibration spectrum, a relative efficiency curve was obtained. These three curves are shown in Figure B.1. This way, the efficiency of the complete system (from fiber aperture to spectrum data file) is known.

The relative efficiency is maximum (i.e. 1) at 586 nm. At the H_α wavelength of 656.3 nm, the relative efficiency of the system is 0.56, while at 486.1 nm (H_β) the relative efficiency is 0.69. The measured $\frac{H_\alpha}{H_\beta}$ ratio therefore has to be multiplied by a factor $\frac{0.69}{0.56} = 1.23$ to compensate for the spectrometer spectral efficiency.
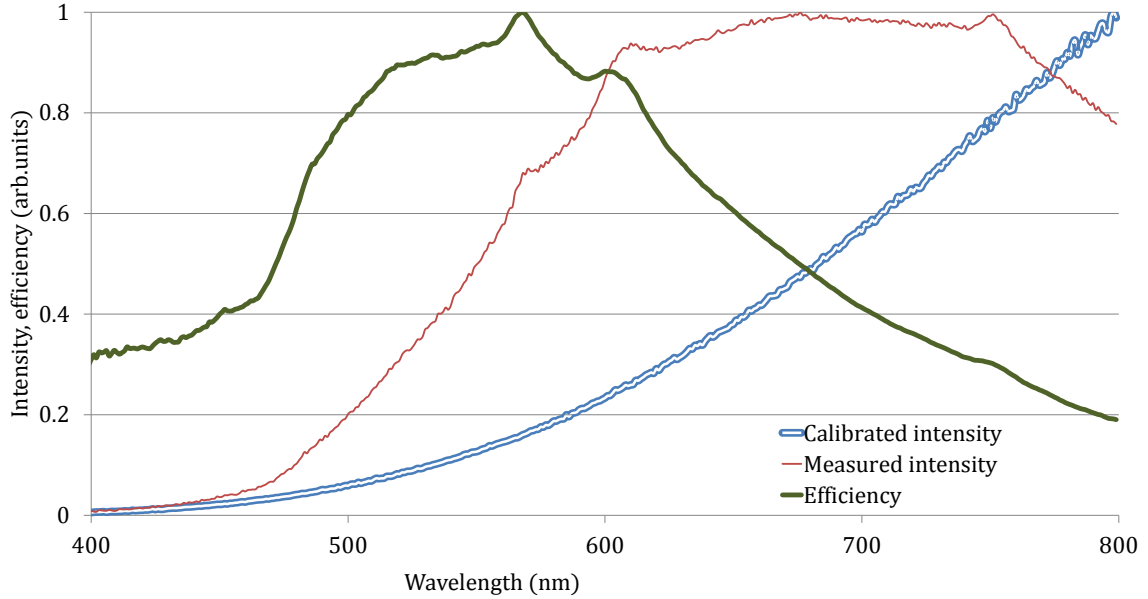

Figure B.1: Comparison of measured halogen spectrum and calibrated spectrum, including relative efficiency curve.

Appendix C

Assignment

The assignment, as proposed by the company mentor, is as follows:

Plasma diagnostics in an inductively coupled H plasma

ASML is the world's leading provider of lithography systems for the semiconductor industry, manufacturing complex machines that are critical to the production of integrated circuits (IC) or microchips. Headquartered in Veldhoven, the Netherlands, ASML designs, develops, integrates, markets and services these advanced systems, which continue to help our customers - the major chipmakers - reduce the size and increase the functionality of microchips, and consumer electronic equipment. ASML has some 10000 employees of which close to 2500 work in R&D. ASML is the only company worldwide that has developed and is selling state-of-the art EUV lithography machines that are the driver for further innovation in IC technology. Some of the capped multilayer mirrors that are used in EUV tools are exposed to intense plasmas. To investigate the effect of these plasmas on the mirrors, a H_2 plasma setup was built at ASML Research. To relate the results obtained with this setup to EUV tool conditions, a thorough study of the plasma conditions in the H_2 plasma setup is essential. Within the proposed internship the student (HBO-level) will participate in the characterization of the inductively coupled H_2 plasma and in upgrades of the system towards conditions that most closely represent the conditions in the EUV tool. In more detail, the student will perform measurements of the residual and undesired capacitively coupled part of the hydrogen plasma in the setup through direct electrical measurements (Langmuir probe related) and indirect measurement of the plasma effects on witness samples. The goal of the project is to reduce the power of the capacitively coupled part of the plasma to a minimum by effectively grounding and shielding the plasma tube. Depending on the progress of the project, the student will be further involved in the plasma characterization by measuring H radical formation in the inductively coupled plasma using spectroscopic techniques.